Three-Dimensional Negative Index of Refraction at Optical Frequencies by Coupling Plasmonic Waveguides

Ewold Verhagen,* René de Waele, L. Kuipers, and Albert Polman
Center for Nanophotonics, FOM Institute for Atomic and Molecular Physics (AMOLF), Science Park 104, 1098 XG, Amsterdam, The Netherlands

(Received 4 May 2010; revised manuscript received 6 October 2010; published 23 November 2010)

We identify a route towards achieving a negative index of refraction at optical frequencies based on coupling between plasmonic waveguides that support backwards waves. We show how modal symmetry can be exploited in metal-dielectric waveguide pairs to achieve negative refraction of both phase and energy. Control of waveguide coupling yields a metamaterial consisting of a one-dimensional multilayer stack that exhibits an isotropic index of -1 at a free-space wavelength of 400 nm. The concepts developed here may inspire new low-loss metamaterial designs operating close to the metal plasma frequency.

DOI: 10.1103/PhysRevLett.105.223901 PACS numbers: 42.25.−p, 42.82.Et, 73.20.Mf, 78.20.Ci

Metamaterials allow control over the propagation of electromagnetic waves in ways beyond those provided by naturally occurring materials. Since the prediction that a material with a negative index of refraction can be used to construct a perfect lens [1], a quest for media that possess a negative index has resulted in a wide range of metamaterials [2]. Many designs of such ''left-handed'' materials are based on metallic resonant scattering elements that exhibit a simultaneously negative electric and magnetic response to light. These geometries can be related to archetypical structures such as split rings at low frequencies, where $\varepsilon_m \ll -\varepsilon_d$ (ε_m and ε_d are the dielectric constants of the metal and its dielectric surrounding, respectively) [2]. However, by using this route it has proven to be difficult to achieve a negative index with acceptable losses at visible frequencies, i.e., close to the metal plasma frequency ω_p [3–5]. Moreover, the desired behavior occurs only for a limited range of angles. In a left-handed medium the direction of energy flow is opposite to the wave vector ($\mathbf{k} \cdot \mathbf{S} < 0$) [6,7]. Preferably, a negative index metamaterial would have a phase index that is independent of angle, with wave vector $\mathbf{k}$ and Poynting vector $\mathbf{S}$ being entirely antiparallel. Both phase and energy are then refracted negatively at an interface of a positive index medium with the metamaterial. Indefinite materials form another class of metamaterials, which can exhibit hyperbolic dispersion, resulting in negative refraction of energy and the conversion of incident evanescent waves to propagating waves [8–11]. However, negatively refracting indefinite materials have a positive phase index (or a negative index with positive refraction), which is moreover strongly angle-dependent.

In this Letter, we propose a strategy to design metamaterials that have a three-dimensional negative index of refraction at visible frequencies, yielding negative refraction of both phase and energy. The working principle relies on coupling between plasmonic waveguides arranged in a stacked geometry. We use the optical properties of metals close to the plasma frequency, where $-\varepsilon_d < \varepsilon_m < 0$, which allow the constituting waveguides to support backwards surface plasmon polariton (SPP) waves [12–17]. We show that the symmetry of the waveguide modes is crucial to the realization of negative refraction in the metamaterial. By exploiting symmetric modes in arrays of equally spaced pairs of plasmonic waveguides, coupling can be tailored to achieve negative refraction of both wave vector and energy. The design strategy presented in this Letter allows the attainment of an isotropic negative index of refraction of -1 for TM-polarized light in a one-dimensional array of plasmonic slab waveguides, operating at visible frequencies with comparatively small absorption losses.

A metamaterial with an isotropic index of refraction n exhibits a spherical isofrequency surface $k_x^2 + k_y^2 + k_z^2 = (n\omega/c)^2$ relating the wave-vector components in three dimensions. We consider a metamaterial comprised of slab waveguides stacked in the z direction (as sketched in the inset in Fig. 1). To find general qualitative requirements on the nature of the modes that such waveguides need to support to achieve all-angle negative refraction of phase and energy, we first consider the paraxial limit of small k_z. There, propagation can be approximated by coupled mode theory, assuming weak coupling [10,18].

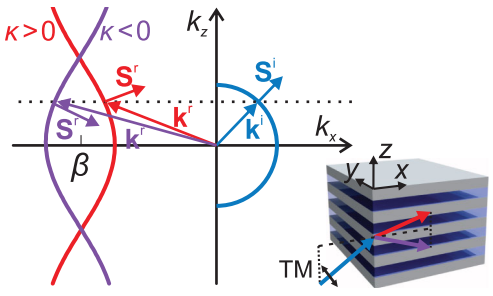

FIG. 1 (color). Wave-vector diagram showing isofrequency contours of a homogeneous positive index medium (blue curve) and left-handed waveguide array with $\kappa > 0$ (red curve) or $\kappa < 0$ (purple curve).

In the xy plane, parallel to the slabs, the isotropy of the structure guarantees the wave vector is independent of angle ($k_x^2 + k_y^2 = \beta'^2$). Its magnitude β' will differ slightly from the mode wave vector β in an isolated waveguide due to interwaveguide coupling. The effective index of refraction in the xy plane is given by $\beta' c/\omega$. For the material to be left-handed, the mode wave vector β of the constituting waveguides must therefore be negative.

A further requirement can be found by analyzing propagation in the xz plane in the paraxial approximation. The amplitudes in adjacent waveguides are related through [18]

$$\partial a_j/\partial x = i\beta a_j + i\kappa(a_{j-1} + a_{j+1}), \tag{1}$$

where a_j is the complex amplitude of the mode in the jth waveguide and κ a coupling constant. Its solution for $k_y = 0$ and center-to-center waveguide separation d is

$$k_x = \beta + 2\kappa\cos(k_z d), \tag{2}$$

sketched in a wave-vector diagram in Fig. 1 for different signs of the coupling constant κ and taking $\beta < 0$. The blue curve indicates the isofrequency contour for a homogeneous positive index medium. Since we will consider refraction of a plane wave incident from $x = -\infty$, only curves are drawn for which $S_x > 0$. By definition, the group velocity (and as we will show in the absence of loss also $\mathbf{S}$) is oriented normal to an isofrequency contour. Given an incident wave vector $\mathbf{k}^i$, the refracted wave vector $\mathbf{k}^r$ can be derived from the diagram by conserving k_z [19]. Figure 1 shows that $\mathbf{k}^r \cdot \mathbf{S}^r < 0$ because $\beta < 0$, and the material is therefore indeed left-handed. Importantly, however, whether the refraction of energy ($\mathbf{S}^r$) is positive or negative is determined by the sign of κ. If $\kappa < 0$, the refraction of energy is negative ($S_z^i S_z^r < 0$), whereas it is positive if $\kappa > 0$. This analysis for small k_z shows that minimum requirements to reach an isotropic negative index are that both β and κ must be negative.

Guided modes with $\beta < 0$ can be called "backwards" since energy and phase are counterpropagating [6]. They exist, for example, in a thin dielectric slab clad with metal [a metal-dielectric-metal (MDM) waveguide] [12–17]. Figure 2 depicts dispersion curves of the propagating SPP modes in a MDM waveguide, calculated with a transfer matrix formalism described in Ref. [17] by using $\varepsilon_m = 1 - \omega_p^2/\omega^2$ and $\varepsilon_d = 2.25$. We neglect absorption here, but as we will see the same physics applies once it is included. The symmetry of the transverse electric field E_z assigns the mode symmetry. The antisymmetric mode acquires a negative group velocity $d\omega/d\beta$ for dielectric thickness $t < (\pi c/2\omega_p)\sqrt{(1+\varepsilon_d)/\varepsilon_d}$, when its cutoff frequency becomes larger than the surface plasmon resonance frequency $\omega_{\mathrm{sp}} = \omega_p/\sqrt{1+\varepsilon_d}$. In the absence of absorption, this means that the energy and phase are counterpropagating. For $\omega_{\mathrm{sp}} < \omega < \omega_p$ the waveguide can be described by the negative effective index $\beta c/\omega$, by using the "mirrored" branch with $\beta < 0$ for energy to propagate forwards [17]. This can lead to negative refraction of light into a MDM waveguide [15,17,20]. This effect is, however, purely two-dimensional, restricted to the waveguide plane.

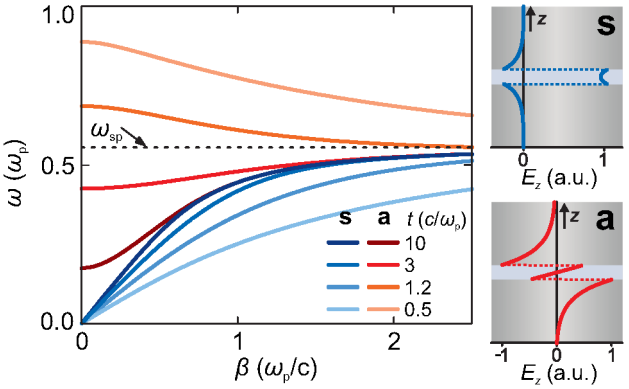

FIG. 2 (color). Dispersion in MDM waveguides, showing the appearance of backwards SPPs for small dielectric thickness t. Characteristic E_z profiles of the symmetric (**s**) and antisymmetric (**a**) SPP modes are shown on the right.

Now we must ensure that these modes, when coupled in a three-dimensional array, lead to a negative coupling constant κ to allow negative refraction of energy in three dimensions. The sign of κ can be found from the modal field in an isolated waveguide since [21]

$$\mathrm{sgn}(\kappa) = \mathrm{sgn}\left(\int_d \mathbf{E}^\dagger(z)\cdot\mathbf{E}(z-d)dz\right), \tag{3}$$

where the mode overlap integral is performed over the dielectric region of the waveguide only. The adjoint field $\mathbf{E}^\dagger$ (obtained by substituting $-\beta$ for β and $-\omega$ for ω) is used to allow for complex ε. Considering $E_z(z)$ of the antisymmetric mode [shown in Fig. 3(a)], we see that $\int_d E_z^\dagger(z)E_z(z-d)dz$ is positive. This is the result of the fact that (i) E_z switches sign across a metal-dielectric interface and (ii) the mode is antisymmetric. Similar reasoning proves $\int_d E_x^\dagger(z)E_x(z-d)dz > 0$ [21]. As a result, a stack of equally spaced MDM waveguides [Fig. 3(b)] will have $\kappa > 0$, exhibiting positive refraction of energy in the xz plane in the paraxial limit, and cannot be used to obtain an isotropic negative index.

As outlined above, the reason that κ is positive is related to the antisymmetric nature of the mode. To achieve negative refraction, a backwards mode with a *symmetric* nature is needed instead. This exists, for example, in a *pair*

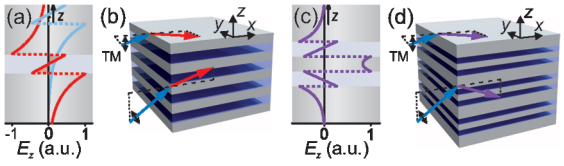

FIG. 3 (color). (a) $E_z(z)$ profile of the antisymmetric mode in a MDM waveguide (red line), together with $E_z(z-d)$ (blue line). (b) Refraction into an array of MDM waveguides. Arrows depict the direction of energy flow. (c) E_z profile of the backwards symmetric mode in a pair of MDM waveguides. (d) Refraction into an array of coupled MDM waveguide pairs.

of strongly coupled MDM waveguides, in which eigenmodes resemble even and odd superpositions of the antisymmetric modes in the individual MDM waveguides. The odd superposition has a negative mode wave vector β that is slightly smaller than that of a single waveguide. Most importantly, this mode has a symmetric overall field profile [see Fig. 3(c), showing that E_z is symmetric with respect to the center of the waveguide pair], which ensures $\kappa < 0$ when we take a pair of MDM waveguides as the basic unit of the array. An array of equally spaced pairs of strongly coupled MDM waveguides, i.e., a metal-dielectric multilayer stack with alternating thick and thin metal layers [Fig. 3(d)], will therefore exhibit negative refraction of energy and wave vector in both the xz and xy planes. An important second advantage to using a symmetric mode is that it can be excited by light incident along $\hat{\mathbf{x}}$, in contrast to antisymmetric modes.

This structure satisfies the requirements on β and κ, which were derived in the paraxial limit and are as such not sufficient to guarantee an isotropic negative index. In order to find out whether it can exhibit a circular isofrequency contour we calculate the wave vector for TM polarization in the metamaterial exactly, by using a transfer matrix method valid for all k_z [19]. The curvature of the isofrequency contour can be controlled by varying the thickness t_m of the metal layer separating adjacent pairs of waveguides, as shown in Fig. 4(a). The free-space wavelength λ_0 is 400 nm. We use the real part of the dielectric constant of Ag ($\varepsilon_m = -4.43$ [22]). We take $\sqrt{\varepsilon_d} = 3.2$, comparable to TiO_2 at this wavelength. A large dielectric index reduces ω_{sp}, extending the operating frequency window to a large part of the visible spectrum. The thicknesses of both dielectric layers and of the thin Ag film are 28 and 35 nm, respectively. Reducing t_m increases the coupling strength, resulting in a stronger modulation of k_x. Interestingly, the isofrequency contours evolve from cosinusoidal [see Eq. (2)] to almost fully circular for $t_m = 75$ nm. The isofrequency surface plotted in a three-dimensional wave-vector diagram [Fig. 4(b)] now resembles a sphere.

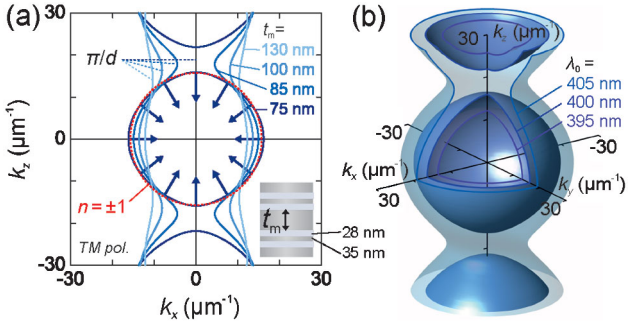

FIG. 4 (color). (a) Calculated wave-vector diagrams for varying metal thickness between waveguide pairs, for the parameters described in the text. The red dotted curve depicts $n = \pm 1$. Arrows show the calculated unit-cell-averaged direction of $\mathbf{S}$ for $t_m = 75$ nm. (b) Three-dimensional wave-vector diagram with isofrequency surfaces for three different values of λ_0.

Wave propagation in the metamaterial can thus be described by an isotropic negative index of refraction n that determines the refraction angle of both the phase and group velocity. At a given frequency, n can be controlled most effectively by changing β through varying the dielectric thickness (see Fig. 2). In this case, it has been chosen such that $n = -1$. The wave-vector magnitude decreases for increasing frequency, showing that the group velocity is oriented inwards. Direct calculation of $\mathbf{S}$ from the fields obtained in the transfer matrix method, depicted by arrows in Fig. 4(a), confirms that it is directed inwards, oriented normal to the isofrequency surface for all wave vectors.

It is interesting to note that, for strong enough coupling, even propagation normal to the interfaces (along $\hat{\mathbf{z}}$) is allowed. The geometry and physical mechanism is different than for metal-dielectric multilayer stacks in the hyperbolic dispersion regime [23]. The existence of transparency windows in metal-dielectric multilayers is well known and can be attributed to resonantly coupled Fabry-Pérot cavities [24]. In the currently proposed system, the Floquet-Bloch wave propagating along $\hat{\mathbf{z}}$ possesses a harmonic in the first Brillouin zone that is described by a negative index [25,26]. Of course, the fact that the wave comprises many harmonics has implications for applications. For example, when used to construct a lens to transfer an image along $\hat{\mathbf{x}}$, the largest wave-vector component k_z that can be transferred is π/d; i.e., the resolution along $\hat{\mathbf{z}}$ is limited by the dimension of a single waveguide. This can, however, be designed to be significantly smaller than $\lambda_0/2$. When introducing realistic absorption losses in the previous example ($\varepsilon_m = -4.43 + 0.21i$ [22]), $\mathrm{Re}(n)$ is not notably affected [21]. The figure of merit, $\mathrm{Re}(|\mathbf{k}|)/\mathrm{Im}(|\mathbf{k}|)$, varies from 14.7 along $\hat{\mathbf{x}}$ to 8.7 along $\hat{\mathbf{z}}$. Considering the fact that λ_0 is only 400 nm, absorption is thus comparatively small [4,5,27] and not strongly dependent on direction.

To illustrate negative refraction of light into the metamaterial, Fig. 5 shows the H_y field in the metamaterial that is illuminated with a TM-polarized plane wave ($\lambda_0 = 400$ nm) incident under a 30° angle from the air. The illuminated interface is normal to the waveguides (along yz) in Fig. 5(a) and parallel to the slabs (along xy) in Fig. 5(b). The material parameters are the same as before, including absorption. Figure 5(a) is calculated with the finite-difference time-domain method, by using a mesh size of 0.5 nm and including absorption in Ag by locally fitting ε_m to a Drude model with dissipation [28]. Figure 5(b) is the result of a transfer matrix calculation. The arrows indicate the calculated unit-cell-averaged direction of $\mathbf{S}$, showing that not only the wave fronts, but indeed also energy is refracted negatively with $n = -1$ for light incident on both interfaces. This is reproduced for different angles [21]. The fraction of energy coupled into the metamaterial is 2% in Fig. 5(a) and 98% in Fig. 5(b). In Fig. 5(a), the remainder of the light is reflected, giving rise to the interference pattern in the left. Simulations show that coupling efficiencies up to 20% are readily available by

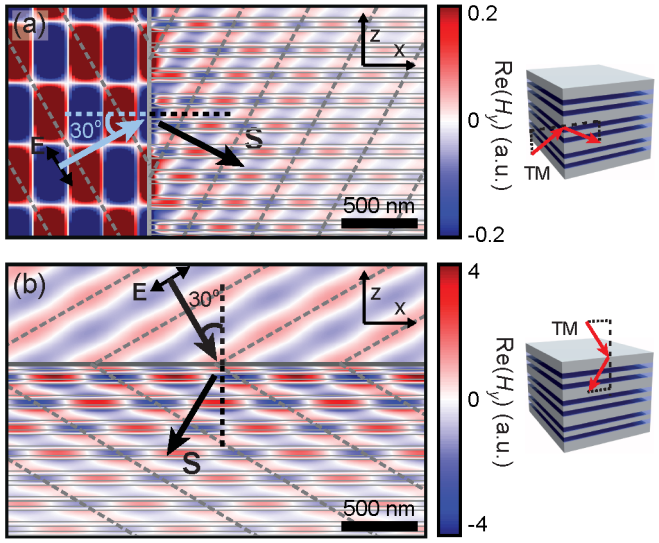

FIG. 5 (color). Snapshots of the H_y field distribution showing refraction of light ($\lambda_0 = 400$ nm) from air into the metamaterial. The arrows show the unit-cell-averaged direction of the time-averaged Poynting vector. The illuminated interface is normal (a) or parallel (b) to the waveguides. Gray dashed lines indicate incident and refracted wave fronts. The color scale is normalized to the incident amplitude; it is saturated in (a) for clarity.

tuning the layer thicknesses [21]. Structuring the interface may further improve impedance matching. Such matching was employed to minimize reflection in Fig. 5(b), by tuning the thickness of the outermost Ag layer to 35 nm [19]. Impedance matching is of particular importance for applications such as lensing. Further studies should identify the degree to which the impedance can be designed to be isotropic as well and the existence of surface waves necessary to amplify evanescent waves. It would be interesting to derive the effective permittivity and permeability for this metamaterial and develop a description valid for all angles that is more intuitive than the transfer matrix method. Such a framework needs to go beyond effective medium theory.

In conclusion, we have identified a route towards the construction of (left-handed) negative index metamaterials by using plasmonic waveguide coupling. We underlined the role of backwards SPP modes and modal symmetry to achieve negative refraction of both the energy and wave vector. A carefully designed one-dimensional stack of metallic and dielectric layers can be characterized by a single three-dimensional isotropic negative index of refraction of $n = -1$ at a wavelength of 400 nm. In this respect, it differs strongly from two-dimensional photonic crystal slabs exhibiting a negative index [25,26,29], in which backward wave behavior relies fully on Bragg diffraction. While it transmits only TM-polarized light, polarization-independent behavior could be found by exploiting alternative waveguide geometries [13,30]. By using Ag, the operating frequency extends from the visible to the near-UV regime, with figures of merit of the order of 10. The same mechanisms can be applied throughout the electromagnetic spectrum, by using conductive oxides in the near-infrared, SiC in the midinfrared, (doped) semiconductors at infrared and terahertz frequencies, and wire-mesh metamaterials in the microwave regime [31]. We envisage that the conceptual framework outlined here may lead to a new class of metamaterial designs exploiting the properties of metals near the plasma frequency.

This work is part of the research program of FOM, which is financially supported by NWO. It is supported by the Joint Solar Programme (JSP) of FOM, which is cofinanced by NWO and Stichting Shell Research.

*Present address: École Polytechnique Fédérale de Lausanne, 1015 Lausanne, Switzerland.
ewold.verhagen@epfl.ch

[1] J. B. Pendry, Phys. Rev. Lett. **85**, 3966 (2000).
[2] C. M. Soukoulis *et al.*, Science **315**, 47 (2007).
[3] R. Merlin, Proc. Natl. Acad. Sci. U.S.A. **106**, 1693 (2009).
[4] G. Dolling *et al.*, Opt. Lett. **32**, 53 (2007).
[5] S. Xiao *et al.*, Opt. Lett. **34**, 3478 (2009).
[6] V. G. Veselago and E. E. Narimanov, Nature Mater. **5**, 759 (2006).
[7] S. Foteinopoulou, E. N. Economou, and C. M. Soukoulis, Phys. Rev. Lett. **90**, 107402 (2003).
[8] D. R. Smith and D. Schurig, Phys. Rev. Lett. **90**, 077405 (2003).
[9] R. Wangberg *et al.*, J. Opt. Soc. Am. B **23**, 498 (2006).
[10] X. Fan *et al.*, Phys. Rev. Lett. **97**, 073901 (2006).
[11] J. Yao *et al.*, Science **321**, 930 (2008).
[12] P. Tournois and V. Laude, Opt. Commun. **137**, 41 (1997).
[13] G. Shvets, Phys. Rev. B **67**, 035109 (2003).
[14] A. Alù and N. Engheta, J. Opt. Soc. Am. B **23**, 571 (2006).
[15] H. Shin and S. Fan, Phys. Rev. Lett. **96**, 073907 (2006).
[16] M. I. Stockman, Phys. Rev. Lett. **98**, 177404 (2007).
[17] J. A. Dionne *et al.*, Opt. Express **16**, 19 001 (2008).
[18] H. S. Eisenberg *et al.*, Phys. Rev. Lett. **85**, 1863 (2000).
[19] P. St. J. Russel, T. A. Birks, and F. D. Lloyd-Lucas, in *Confined Electrons and Photons*, edited by E. Burstein and C. Weisbuch (Plenum, New York, 1995).
[20] H. J. Lezec *et al.*, Science **316**, 430 (2007).
[21] See supplementary material at http://link.aps.org/supplemental/10.1103/PhysRevLett.105.223901, which discusses the sign of κ, absorption, and coupling efficiency.
[22] P. B. Johnson and R. W. Christy, Phys. Rev. B **6**, 4370 (1972).
[23] S. A. Ramakrishna *et al.*, J. Mod. Opt. **50**, 1419 (2003).
[24] M. Scalora *et al.*, J. Appl. Phys. **83**, 2377 (1998).
[25] M. Notomi, Phys. Rev. B **62**, 10 696 (2000).
[26] S. Foteinopoulou and C. M. Soukoulis, Phys. Rev. B **67**, 235107 (2003).
[27] J. Valentine *et al.*, Nature (London) **455**, 376 (2008).
[28] Lumerical FDTD SOLUTIONS 6.
[29] S. Foteinopoulou and C. M. Soukoulis, Phys. Rev. B **72**, 165112 (2005).
[30] S. P. Burgos *et al.*, Nature Mater. **9**, 407 (2010).
[31] J. B. Pendry *et al.*, Phys. Rev. Lett. **76**, 4773 (1996).